# Solution structure of protegrin-1, a broad-spectrum antimicrobial peptide from porcine leukocytes

Richard L Fahrner[1], Thorsten Dieckmann[1], Sylvia SL Harwig[3], Robert I Lehrer[2,3], David Eisenberg[1,2] and Juli Feigon[1,2]

**Background:** The protegrins are a family of arginine- and cysteine-rich cationic peptides found in porcine leukocytes that exhibit a broad range of antimicrobial and antiviral activities. They are composed of 16–18 amino-acid residues including four cysteines, which form two disulfide linkages. To begin to understand the mechanism of action of these peptides, we set out to determine the structure of protegrin-1 (PG-1).

**Results:** We used two-dimensional homonuclear nuclear magnetic resonance spectroscopy to study the conformation of both natural and synthetic PG-1 under several conditions. A refined three-dimensional structure of synthetic PG-1 is presented.

**Conclusions:** Both synthetic and natural protegrin-1 form a well-defined structure in solution composed primarily of a two-stranded antiparallel β sheet, with strands connected by a β turn. The structure of PG-1 suggests ways in which the peptide may interact with itself or other molecules to form the membrane pores and the large membrane-associated assemblages observed in protegrin-treated, gram-negative bacteria.

Addresses: [1]Department of Chemistry and Biochemistry, [2]Molecular Biology Institute, and [3]Department of Medicine, University of California, Los Angeles, CA 90095, USA.

Correspondence: Juli Feigon
e-mail: feigon@ewald.mbi.ucla.edu

**Key words:** antibiotic, leukocytes, protegrin, antiviral; two-dimensional NMR

Received: **7 May 1996**
Revisions requested: **24 May 1996**
Revisions received: **24 Jun 1996**
Accepted: **25 Jun 1996**

**Chemistry & Biology** July 1996, **3**:543–550

 ISSN 1074-5521

## Introduction

Protegrins are a family of peptides isolated from porcine leukocytes [1], that have a broad range of antimicrobial and antiviral activities. Five of these peptides have been identified to date [1–3]. The protegrins are active against several gram-positive and gram-negative bacteria [1,4] and against chlamydiae [5], mycobacteria [6] and HIV-1 [7]. Protegrins and analogous antimicrobial peptides are thought be important in defending various tissues from infection, in part by augmenting the oxidative microbicidal pathways operative in leukocytes [8]. The protegrins are composed of 16–18 amino-acid residues including four invariant cysteine residues, which form two disulfide bonds [9]. (See Fig. 1 for the sequence of PG-1 and the arrangement of the disulfide bridges.) Their amino-acid sequences and compositions are similar to those of certain defensins [1], another family of antibiotic peptides [10], and they bear a striking resemblance to tachyplesins, a family of antimicrobial peptides obtained from the hemocytes of horseshoe crabs [11]. These similarities include a mostly β sheet structure and a high content of cysteine and basic residues.

Due to their small size, potent antimicrobial activity, and wide range of susceptible targets, protegrins are attractive model compounds for use as pharmacological agents. We set out to determine the structure of these compounds as a first step in understanding the mechanism of action of these peptides, and to provide a basis for further development of modified protegrins as drugs.

Here, we present homonuclear NMR studies of PG-1 isolated from porcine leukocytes (natural PG-1) and synthetic PG-1. Both peptides form a similar well-defined structure under the conditions examined, although there was an additional minor conformation present in natural PG-1. A refined three-dimensional structure of synthetic PG-1 is presented. The peptide forms a two-stranded anti-parallel β sheet along nearly its entire length, with

**Figure 1**

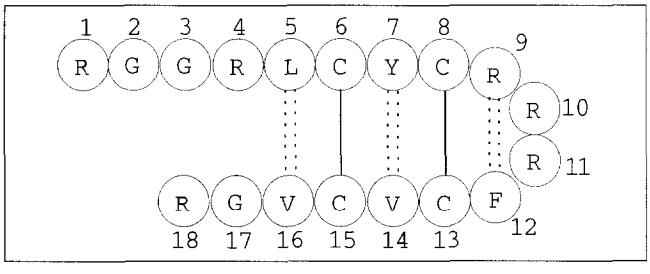


Sequence and numbering system of porcine protegrin-1 (PG-1). The disulfide linkages (solid lines) and proposed pattern of cross-strand hydrogen bonds (dashed lines), deduced from the NMR data, are indicated. The carboxy-terminal residue of natural PG-1 (Arg18) is amidated.

strands joined by a β turn, resembling a hairpin. The disulfide bonds are in a parallel arrangement, as had been predicted previously [9]. Based on the structure of protegrin, we discuss how this peptide might disrupt the membranes of microorganisms.

## Results

### Synthetic PG-1 forms a β sheet

The spin systems in synthetic PG-1 were identified from double quantum filtered correlation spectroscopy (DQF-COSY) [12] (not shown) and total correlation spectroscopy (TOCSY) [13] spectra (Fig. 2). The sequence-specific assignments were then obtained from the sequential connectivities observed in the amide–alpha and amide–amide crosspeak regions of the spectrum obtained by nuclear Overhauser enhancement spectroscopy (NOESY) [14] (Fig. 3a,b) using the aromatic residues as an initial starting point. To resolve ambiguities in assignment from spectral overlap, all spectra were acquired at both 1 °C and 20 °C. The sequential connectivities observed are summarized in Figure 4, and the proton assignments are given in Table 1.

**Figure 2**

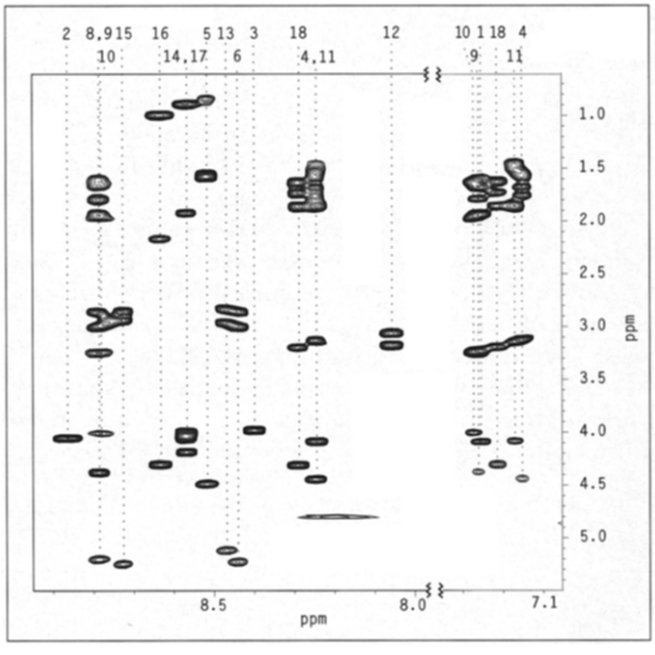


Sidechain assignments of PG-1. A portion of a TOCSY spectrum ($\tau_m$ = 80 ms) is shown of 2 mM synthetic PG-1 (TFA form) in 90 % $H_2O$/10 % $D_2O$, 10 mM sodium phosphate, pH 6.5 at 20 °C showing the crosspeaks from the sidechain spin systems to the amide protons (left) and arginine ϵ protons (right). Intra-sidechain connectivities are indicated by dashed lines and labeled at the top. The spectrum was acquired with 2048 and 600 points in $\omega_2$ and $\omega_1$, respectively, and a recycle delay of 1.3 s. The spectrum was zero-filled to 2048 points in both dimensions and apodized with a Gaussian multiplication with Lorentzian broadening (LB) of −18 and Gaussian broadening (GB) of 0.1 in $\omega_2$ and LB of −18 and GB of 0.18 in $\omega_1$.

**Figure 3**

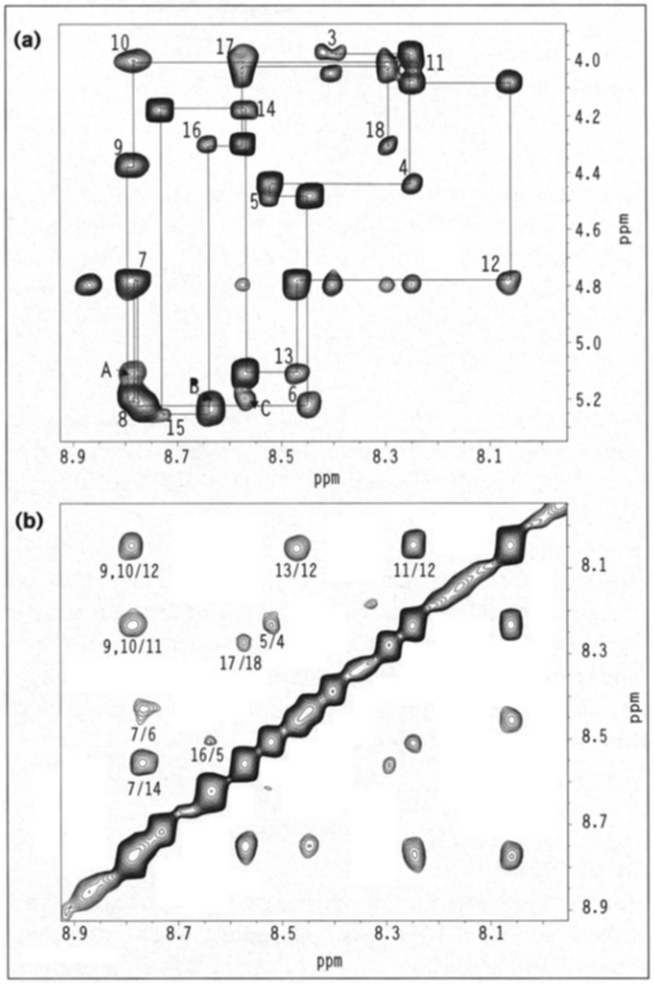


NMR spectroscopy of synthetic PG-1 indicates that it forms a β sheet. Portions of a NOESY spectrum ($\tau_m$ = 300 msec) of 4 mM synthetic PG-1 (acetate form) in 90 % $H_2O$/10 % $D_2O$ in 10 mM sodium phosphate, pH 6.5 at 20 °C. **(a)** Amide–alpha (fingerprint region). Sequential connectivities are indicated by solid lines. Additional NOEs identified are (A) 7NH–13$C_\alpha$H, (B) 16NH–6$C_\alpha$H and (C) 14NH–8$C_\alpha$H. **(b)** Amide–amide region. Sequential and long range crosspeaks are labeled. Ambiguities in the assignments for overlapped peaks were resolved in spectra taken at other temperatures. The spectrum was acquired with 2048 and 600 points in $\omega_2$ and $\omega_1$, respectively, and a recycle delay of 1.3 s. The spectrum was zero-filled to 2048 points in both dimensions and apodized with a Gaussian multiplication with LB of −18 and GB of 0.12 in $\omega_2$ and 75° phase-shifted squared sinebell in $\omega_1$.

Strong $C_\alpha H_i$–$NH_{i+1}$ and weaker $NH_i$–$NH_{i+1}$ crosspeaks were observed from residues 2–9 and 12–17, indicating that the peptide chain has an extended structure [15]. The $^3J_{\alpha N}$ couplings for residues 6, 8, 9, and 13–16 were larger than 8.5 Hz, which is also consistent with an extended conformation [15]. In addition to the sequential nuclear Overhauser effect (NOE) crosspeaks, several long range NH–$C_\alpha$H (Fig. 3a), NH–NH (Fig. 3b), and $C_\alpha$H–$C_\alpha$H NOEs (4 to 17 and 8 to 13) were identified for residues 4–17. These long-range NOEs establish that PG-1 folds

**Figure 4**

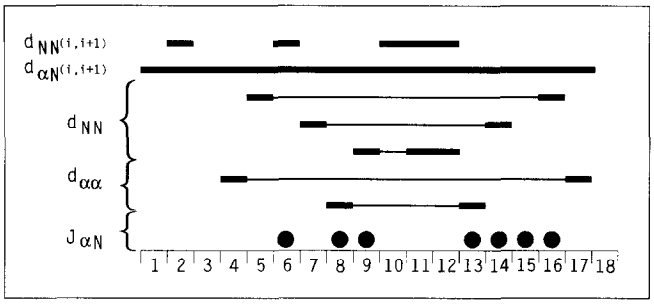


Summary of sequential and long-range NOEs observed for synthetic PG1 (acetate form). A bar indicates that an NOE was observed. For long range NOEs, bars are connected by a thin line to indicate that an NOE was oberved between them. Strong coupling ($J_{\alpha N} > 8.5$ Hz) is indicated by a black circle.

into an antiparallel β sheet along almost its entire length [15], from residues 4 to 8 and 13 to 17. Additional NOEs in the loop region (residues 9–12) indicate that a β turn is formed. Since the pattern of NOEs observed fits several types of β turns, we cannot classify the specific type of β turn from the NMR data [15]. In all of the low energy structures calculated, however, this turn is a type II β turn.

### Natural PG-1 contains a minor conformation

NOESY spectra of the acetate salt of natural PG-1 exhibit crosspeak patterns and relative intensities that are the same as for the acetate salt of synthetic PG-1. In the natural sample, however, we observed a few additional NOE crosspeaks in the fingerprint region. These include four additional intra-residue Cys amide–alpha crosspeaks and several sequential amide–alpha crosspeaks to the four Cys residues. A portion of a TOCSY spectrum of natural PG-1 (acetate form) is shown in Figure 5, illustrating the four additional Cys amide–alpha crosspeaks. Crosspeaks from this minor conformer are also present in spectra of the trifluoroacetate (TFA) salt of natural PG-1, but not in spectra of the TFA salt of synthetic PG-1. No other crosspeaks from the minor conformation are observed in the TOCSY spectra. Based on the chemical shift of these peaks, the sequential amide–alpha crosspeaks, and the lack of any additional peaks in the spectra, we believe that the additional NOEs indicate that an alternative conformation of the Cys residues is present in natural protegrin. By comparing the relative intensities of the crosspeaks, we estimate that ~10 % of the PG-1 in the natural sample is in the minor conformation.

### PG-1 is a monomer in solution

Samples of natural protegrin were originally obtained as the TFA salt, whereas those of the synthetic peptide were purified as the acetate salt. Although similar spectra were obtained from both samples, NOESY spectra of the natural protegrin (TFA form) had far fewer inter-residue NOEs than spectra from the synthetic sample (acetate form). If natural protegrin was reformulated as the acetate salt, however, the spectra obtained were identical to those of the synthetic protegrin, except for the additional crosspeaks arising from the minor conformation. Furthermore, synthetic protegrin prepared as the TFA salt gave spectra identical to those of the TFA salt of natural protegrin, except for the crosspeaks arising from the minor conformation. Thus, the differences in NOEs observed in the spectra between the various samples arose from the counterion used during purification.

**Table 1**

**$^1$H chemical shifts in ppm of acetate form of synthetic PG-1 at 20 °C in 10 mM Na phosphate, pH 6.5.**

| Residue | NH | α | β | γ | δ | ε |
|---|---|---|---|---|---|---|
| 1 Arg | 8.78 | 4.09 | 1.95* | 1.69* | 3.24* | 7.25 |
| 2 Gly | 8.86 | 4.05 | – | – | – | – |
| 3 Gly | 8.39 | 3.97 | – | – | – | – |
| 4 Arg | 8.24 | 4.44 | 1.69, 1.76 | 1.55, 1.59 | 3.13* | 7.14 |
| 5 Leu | 8.51 | 4.48 | 1.53* | 1.58* | 0.83, 0.88 | – |
| 6 Cys | 8.44 | 5.23 | 2.85, 3.00 | – | – | – |
| 7 Tyr | 8.76 | 4.80 | 2.96* | – | – | – |
| 8 Cys | 8.78 | 5.20 | 2.86, 2.99 | – | – | – |
| 9 Arg | 8.78 | 4.38 | 1.79, 1.93 | 1.59, 1.68 | 3.26* | 7.25 |
| 10 Arg | 8.78 | 4.00 | 1.98* | 1.64* | 3.26* | 7.25 |
| 11 Arg | 8.24 | 4.08 | 1.87* | 1.47, 1.51 | 3.16* | 7.16 |
| 12 Phe | 8.05 | 4.80 | 3.07, 3.18 | – | – | – |
| 13 Cys | 8.46 | 5.12 | 2.85, 2.97 | – | – | – |
| 14 Val | 8.56 | 4.18 | 1.938 | 0.88* | – | – |
| 15 Cys | 8.72 | 5.25 | 2.85, 2.94 | – | – | – |
| 16 Val | 8.63 | 4.30 | 2.17* | 0.99* | – | – |
| 17 Gly | 8.56 | 4.03 | – | – | – | – |
| 18 Arg | 8.28 | 4.31 | 1.74, 1.86 | 1.64* | 3.20* | 7.21 |

A hyphen indicates that a proton type is not applicable. An asterisk indicates that the chemical shifts for geminal protons are degenerate.

**Figure 5**

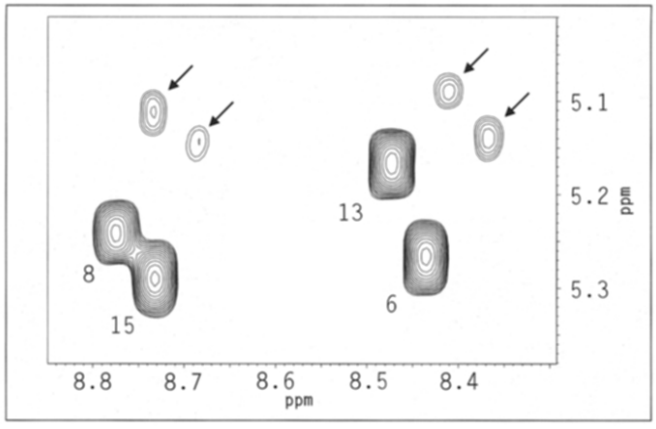


Natural PG-1 forms the same structure as synthetic PG-1 but also contains a minor conformation. The TOCSY spectrum of the Cys amide–alpha region of natural PG is shown. Crosspeaks arising from the minor conformation are labeled by arrows. The spectrum was acquired with 2048 and 800 points in $\omega_2$ and $\omega_1$, respectively and a recycle delay of 2 s. The spectrum was zero-filled to 2048 points in both dimensions and apodized with a Gaussian multiplication with LB of −15 and GB of 0.12 in $\omega_2$ and 75 phase-shifted squared sinebell in $\omega_1$.

To determine whether this difference between the TFA and acetate forms of PG-1 might be due to oligomerization in the presence of one counterion and not the other, we made NMR diffusion measurements on both samples [16] (data not shown). Based on the results of these experiments and the absence of data in the NMR spectra that would support oligomeric association, we conclude that PG-1 is monomeric in the solution conditions examined.

### Three-dimensional structure of synthetic PG-1

We generated 100 structures from the combined distance geometry [17] and simulated annealing calculations [18], 73 of which had converged to sufficiently low energies. The structures are based on a total of 221 inter-proton distance restraints determined from NOE crosspeak intensities and 7 ϕ-angle restraints based on $^3J_{\alpha N}$ values (see Table 2). The 20 lowest-energy structures of PG-1 were used for the final analysis.

Stereo views of a superposition of this family of structures are shown in Figure 6a. Most of the structure is unusually well defined for a small peptide, with an overall backbone root mean squared deviation (RMSD) of 2.61 Å. As expected from the NOE crosspeak patterns, PG-1 forms an anti-parallel β sheet from residues 4–8 and 13–17 connected by a β turn. The RMSD for the backbone atoms of residues 4–17 is 0.80 Å. The amino and carboxyl termini (residues 1–3 and 18) have relatively few inter-residue NOE restraints, and thus it is not surprising that these regions appear to be completely unstructured after refinement. Within the well-defined β sheet region, the cross-strand NOE patterns that we observed in the NOESY spectra are consistent with a regular pattern of hydrogen bonds typical for antiparallel β sheets (see Fig. 1). The cysteine cross bridges are generally in either of two conformations, which could not be distinguished in

**Table 2**

**Refinement statistics for synthetic PG1 (acetate form).**

| | |
|---|---|
| **Distance restraints** | |
| Sequential | 60 |
| i, i+2 | 29 |
| i, i+3 | 5 |
| i, i+4 | 3 |
| Long range | 27 |
| Total inter-residue | 124 |
| Intra-residue | 97 |
| Total NOEs | 221 |
| H-bonding restraints | 12 |
| Dihedral angle restraints (ϕ = 120° ± 30°) | 7 |
| **Restraint violations** | |
| NOE violations > 0.5 Å | 0 |
| NOE violations > 0.2 Å | 5.3 |
| Dihedral angle violations | 0 |

**Convergence**

| | All residues (1–18) | β sheet and loop (4–17) | β sheet (4–8, 13–17) | Loop (9–12) |
|---|---|---|---|---|
| Backbone (RMSD) | 2.61 (±0.95) Å | 0.80 (±0.50) Å | 0.61 (±0.52) Å | 0.49 (±0.54) Å |
| All heavy atoms (RMSD) | 3.80 (±0.94) Å | 2.29 (±0.70) Å | 1.79 (±0.64) Å | 2.24 (±0.87) Å |

Violations are the average number of violations per structure for the 20 lowest energy structures. Values given under convergence are pairwise RMSD values ± standard deviation.

**Figure 6**

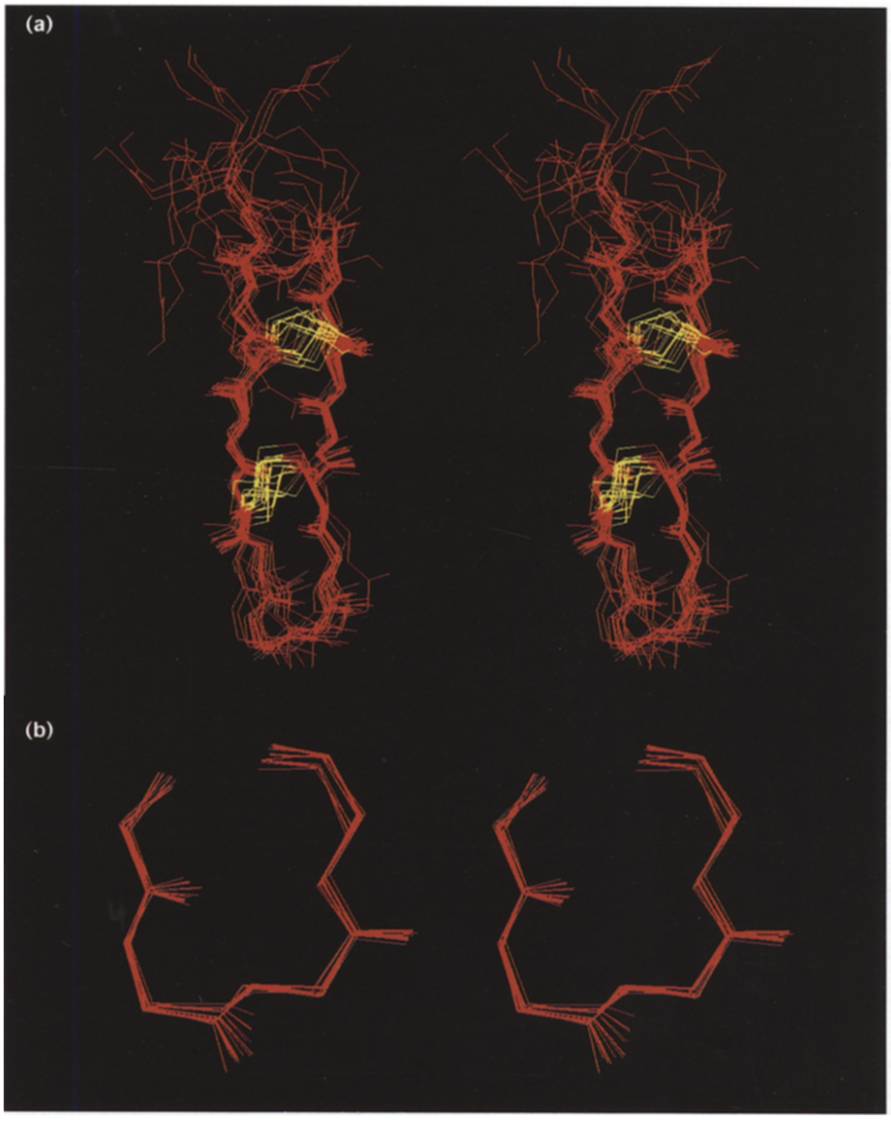


Stereoviews of the 20 lowest energy refined three-dimensional structures of synthetic PG-1 (acetate form) in 10 mM sodium phosphate, pH 6.5. **(a)** Backbone (heavy atoms only) of PG-1, illustrating the anti-parallel β sheet (red) and cysteine cross bridges (yellow). Residues 4–17 were superimposed. **(b)** Loop residues 8–13 of PG-1, illustrating the β turn structure. Residues 9 through 12 were superimposed.

the absence of stereospecific assignments of the β protons. (These could not be stereospecifically assigned because of spectral overlap.) The sidechains of Leu5, Tyr7, Phe12, Val14,16 all extend above the plane of the β sheet, forming a relatively well ordered apolar cluster. Although the backbone of the β sheet region is well-defined, the sidechains of the arginine residues are much less well defined and appear to be highly mobile.

In the stereoview of the complete peptide backbone (Fig. 6a), the turn region (residues 9–12) appears to be less well-defined than the β sheet region. A superposition of only the residues in the turn region (Fig. 6b), however, demonstrates that the local structure of the turn is, in fact, well defined, and the larger RMSD values in this region are mainly due to a 'hinge movement' of the turn region, relative to the β sheet.

The appearance of the structure of protegrin may be qualitatively described as an extended ellipsoid, ~30 Å long and ~8 Å in cross section (shown in Fig. 7 from four angles of view). It is interesting to note that polar and apolar sidechains are segregated; the arginine residues (with charged nitrogen atoms shown in dark blue) are found toward the ends of the long axis; apolar methylene and other carbon-containing groups (shown in light green) and disulfide bonds (in dark green) are toward the center of the molecule.

## Discussion

### Comparison with structures of related proteins

PG-1 is similar in structure to tachyplesin I [19], an antibiotic peptide that belongs to a family of peptides obtained from horseshoe crab hemocytes [11]. Both molecules fold into a two-stranded, anti-parallel β sheet

**Figure 7**

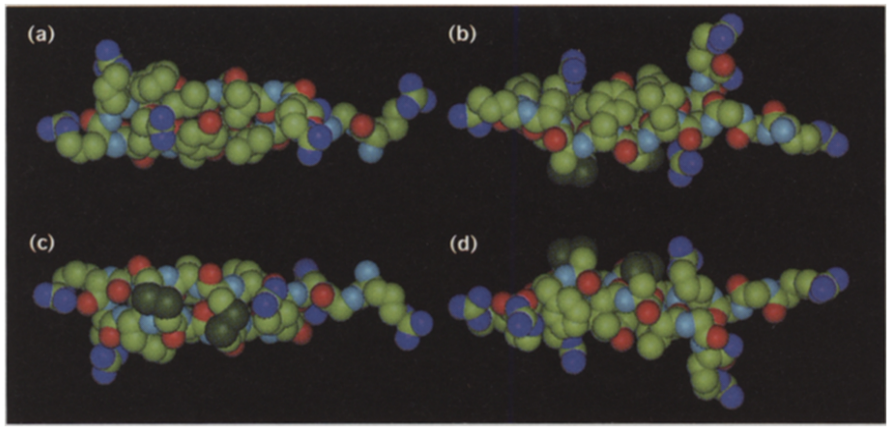


Four views of a space-filling representation of one structure of PG-1, shown as successive rotations of 90° about the horizontal axis. In all views the turn (residues 9–12) is on the left and the tails (residues 1–4 and 17–18) are on the right. **(a)** Top view, with the two disulfide bridges (dark green) facing the viewer; **(b)** Front view, with residues 5–12, among others, facing the viewer (notice the disulfide bonds on top); **(c)** Back view, with residues 12–18, among others, facing the viewer (notice the disulfide bonds on the bottom); **(d)** Bottom view, with the disulfide bonds away from the viewer. The atom colors are as follows: carbon, light green; sulfur, dark green; oxygen, red; uncharged nitrogen, light blue; charged nitrogen, dark blue. Notice that the center of the molecule is relatively apolar (carbon and sulfur groups) whereas the ends of the molecule are highly charged (charged nitrogen). PG-1 contains no charged oxygen. Notice also in the back and front views (panels (b) and (c)) that the array of carbonyl and amino groups offers the possibility of PG-1 hydrogen bonding to other molecules as a β sheet. The charged arginine sidechains also offer the possibility of hydrogen-bonding and electrostatic interactions.

with strands connected by a β turn, and are constrained by two disulfide bonds. However, the distribution of polar and apolar residues in tachyplesin and protegrin is different. In tachyplesin, several polar sidechains and the apolar disulfide bridges extend to one side of the β sheet while the other side of the β sheet contains the apolar sidechains [19]. In contrast, the central portion of the β sheet in PG-1 contains only apolar residues on both surfaces, and the charged residues are clustered in the turn region and in the tails (see Fig. 7). Defensins, which are another family of cationic, cysteine-rich, antibiotic peptides of about twice the molecular weight of protegrins and tachyplesins, form a three-stranded, anti-parallel β sheet. These peptides dimerize along the edges of the β sheet forming a continuous six-stranded β sheet [20]. Apolar sidechains are exposed on one side of the central β sheet region of defensin, whereas the other face contains both apolar and polar residues. The charged residues in defensin are mostly localized at either end of the molecule.

#### Models for the action of protegrins

The antimicrobial activity of the protegrins seems to be based on their ability to form lesions in microbial membranes that lead to rapid microbe death [21]. Protegrin-treated gram-negative bacteria (*Escherichia coli* and *Neisseria gonorrhoeae*) manifest structural lesions that include small breaks in their inner membranes, and, on their outer membranes, multiple elevated circular plaques (~80–100 nm in diameter) with central depressions [4,21]. As no enzymatic function or single specific receptor is known for the protegrins, it seems likely that the actions of protegrins are a consequence of physical interaction with membrane components, probably including charged lipids. Given the solution structure of PG-1 determined here, we suggest three possible modes of physical interaction of protegrins in the destruction of membranes of microorganisms.

The first possible mode of action of protegrin is the formation of an oligomeric structure that creates a membrane pore in the microorganism. This type of model is similar to the model suggested for the action of defensins [20]. There are at least three ways in which PG-1 could associate with itself to form an oligomer. The first two involve self-association of protegrin to form anti-parallel or parallel β sheets between monomers through the backbone amino and carbonyl hydrogen bond donors and acceptors on the sides of the molecule (visible in Fig. 7b,d). The β sheets can associate in two ways: turn-next-to-turn or turn-next-to-tail. Models have been built of these extended protegrin sheets, and both forms place positively charged arginine residues close to other arginine residues on the neighboring PG-1 molecules, almost certainly creating large electrostatic repulsion. Oligomeric association of protegrin could also take place by face to face stacking of the most apolar surfaces of PG-1 molecules (Fig. 7a,d). But models of this mode of association also show that positively charged arginine residues on neighboring molecules are close together. As each of these three hypothetical schemes for associating protegrins probably produces large electrostatic repulsion, we find it difficult to build an electrostatically reasonable model of oligomeric protegrin, at least when protegrin is isolated from other cellular components. In association with lipid or other negatively charged biomolecules, however, stable oligomeric assemblages of protegrin might be able to form.

The second possible mode of action is the binding of individual protegrin molecules to the membrane surface.

PG-1 offers seven positive charges that can interact with the phosphate head groups of lipids. It has been suggested that the guanidinium ion of the arginine sidechain is capable of interacting with two phosphate groups [22]. Conceivably, a PG-1 molecule could bind within the top leaflet of a lipid bilayer, interacting with several phosphate head groups, with its apolar surface (Fig. 7a) facing apolar groups on the lipid. It has been suggested that the α-helical peptide melittin, the main protein component of bee venom, disrupts membranes by binding within one leaflet of a bilayer [23]. Although melittin is helical and PG-1 is a β sheet, PG-1 has molecular dimensions that are comparable to those of melittin. It also has a charge distribution that is similar to that of melittin; positive charges are found at the ends of the long molecular axis, with apolar groups toward the center. Thus protegrins, like melittin, might destabilize membranes by binding initially as individual molecules in the top leaflet of the bilayer.

The third possible mode of action of protegrin is through depletion of lipid from the cell membrane by binding to the lipid components and forming mixed protegrin–lipid micelles. In this model, the membrane would be disrupted by lipids leaving the membrane to interact preferentially in micelles with protegrin. This model would be consistent with the observation of elevated outer-membrane plaques adjacent to membranes in gram-negative bacteria that have been subjected to PG-1 [4]. At present, we speculate that both the second and third possible modes of action are possible for protegrin, and suggest that further experiments, such as an examination of the NMR structure of protegrin in a lipid environment, may allow these two possibilities to be distinguished.

## Significance

**Chemically diverse peptide antibiotics that can destroy a broad range of microbial and viral pathogens are synthesized by many types of animals and animal cells, and have been found in protozoans [24], invertebrates [25], amphibia [26], birds [27], and mammals [1,10]. PG-1, the peptide characterized in this report, has remarkably potent antimicrobial and antiviral properties. Given its small size and relatively simple structure, it provides an attractive template for designing potentially useful chemoprotective peptides. Protegrins also have potential as powerful probes for examining the interactions between β sheet peptides and the cellular membranes of diverse microbial, viral, and eukaryotic targets. A first step in elucidating the mode of action of these peptides is to determine their three-dimensional structure. Here, we have shown that PG-1 forms a well-defined, rigid β sheet structure with the potential to interact with membrane lipids. Both synthetic and natural protegrin form the same structure in solution. This structure thus provides a starting point for structure-based design of chemically modified synthetic protegrins, which may eventually lead to even more potent antimicrobial agents.**

## Materials and methods

*Protegrin synthesis, refolding and purification*

Natural PG-1 was isolated from porcine leukocytes as previously described [1]. Synthetic PG-1 was synthesized using F-moc chemistry and folded [5]. Samples containing either TFA or acetate counterion were purified by fast protein liquid chromatography (FPLC) on a C18 reverse-phase column as follows: for the TFA form, 0.1 % TFA in $H_2O$ was used to bind the PG-1 to the column, and it was eluted with a 0–60 % acetonitrile gradient over 60 min. The acetate form was prepared either by using an initial binding buffer of 0.1 % acetic acid (Intrabiotics Pharmaceuticals, Sunnyvale, CA), or by first following the protocol as described for the TFA form followed by successively drying and redissolving the product three times in 0.1 % acetic acid. Purified PG-1 was stored as a lyophilized powder.

NMR samples were prepared by dissolving the lyophilized PG-1 in water containing the desired salts at concentrations of 2–4 mM peptide. Initially, NMR spectra were obtained on samples of synthetic PG-1 (acetate form), synthetic PG-1 (TFA form), natural PG-1 (acetate form) and natural PG-1 (TFA form) in the following conditions: pH 5.5 in water or 10 mM sodium phosphate pH 5.0, pH 5.5, pH 6.0, pH 6.5 or pH 7.0. For the synthetic PG-1 sample used for the structure calculations, the sample conditions were 4 mM PG-1 in 10 mM sodium phosphate, pH 6.5, 500 μl. Samples were initially prepared in 90 % $H_2O$/10 % $D_2O$ and exchanged to $D_2O$ by repeated drying and redissolution in 99.996 % $D_2O$.

*NMR spectroscopy*

All $^1H$ NMR spectra were obtained at 500 MHz on a Bruker AMX500 spectrometer. For each sample, two-dimensional NMR spectra were acquired at 1 °C and 20 °C as follows: for the sample in $D_2O$, Clean City TOCSY [14], with 80 ms mixing time, and NOESY [12], with presaturation pulse on HDO with mixing times of 300 ms and 150 ms, and for the sample in $H_2O$ (90 % $H_2O$/10 % $D_2O$), Clean City TOCSY, with 80 ms mixing time, DQF-COSY [13] and NOESY, with WATERGATE [28] observe pulse and 300 and 150 ms mixing time.

*NMR diffusion measurements*

Gradient longitudinal eddy current delay experiments [16] were used to estimate the translational diffusion coefficient of PG-1. One-dimensional $^1H$ spectra with gradient lengths between 1.5 and 20 ms were acquired, and the intensity of several different proton resonances were plotted against gradient length. These data were used to determine the state of PG-1 in solution (i.e., monomer, dimer, or higher order aggregate). Several reference molecules of known size were used to calibrate the results.

*$^1H$-NMR assignments of PG-1*

The amino-acid spin systems of PG-1 were identified using the DQF-COSY and TOCSY spectra obtained at 1 °C and 20 °C (Fig. 2). Sequence-specific assignments were obtained by analysis of NOESY spectra (Fig. 3a,b) using standard sequential assignment protocols [15]. Proton resonance assignments were obtained for all of the amino-acid spin systems of PG-1 in both the TFA and acetate forms (Table 1).

*Restraints used in structure calculations*

The NOE restraints were derived from 2D NOESY spectra of PG-1 in $D_2O$ at 20 °C and in $H_2O$ at 1 °C and 20 °C. The crosspeak intensities were integrated using the program AURELIA (Bruker Instruments, Inc.). Where integration was not feasible due to spectral overlap, the crosspeaks were classified qualitatively as strong (2.8 Å), medium (3.5 Å) or weak (5 Å). Crosspeak intensities were translated into distances based on a reference crosspeak originating from Phe12

(2,6–3,5 crosspeak) of 1.9 Å, using the $r^{-6}$ relation. The obtained distances were used with an upper bound of +1.5 Å plus pseudoatom corrections (1.0 Å for $CH_2$ and $CH_3$ and 2.0 Å for aromatic protons) where applicable. The lower bound was set to the van der Waals radius. Additional distance restraints representing hydrogen bonds were introduced for the three cases where a complete set of inter-residue NOEs indicated the existence of a stable hydrogen bond (Fig. 1). Each hydrogen bond was represented by two distances (NH–O and N–O).

An initial set of structures was calculated using only the experimentally derived data (NOE-distance restraints and dihedral-angle restraints). In all of the low energy structures in this initial set, the region between residues 4–9 and 12–17 were in a β sheet conformation with several amide protons and carbonyl oxygens within hydrogen-bonding distance. All amide protons in PG-1 exchange rapidly when transferred into $D_2O$; however, based on the NMR data and the initial structure calculations, hydrogen-bonding constraints were added in those regions where antiparallel β sheet structure was supported by both the NMR and structure calculation data.

Dihedral-angle restraints were estimated based on the NH–CαH J-couplings observed in a DQF-COSY spectrum. In those cases where the coupling was resolved and was larger than 8.5 Hz (seven residues), the ϕ-angle was restricted to a range typical for an extended conformation (−120° ± 30°) [15].

### *Structure calculations*

The structure calculations were performed with the program X-PLOR 3.1, using a combined distance geometry and simulated annealing protocol [18]. The complete set of NOE restraints, H-bond restraints, and dihedral angle restraints was used during all stages of the calculations. 100 starting structures were generated using the distance geometry sub-structure embedding method. All 100 structures were carried through all the following steps. The simulated annealing structure refinement was carried out in three stages: (1) a primary refinement of the starting structure (5000 steps at 2000 °K and 10 000 steps of cooling to 100 °K using a time step of 1 fs), (2) an intermediate refinement (4 cycles of 5000 steps, cooling from 2000 °K to 100 °K with a time step of 2 fs), and (3) a final room temperature refinement (20 000 steps at 300 °K with a time step of 0.5 fs). During the primary refinement only, the disulfide bonds were deleted and replaced by NOE-type distance restraints. The resulting structures were sorted by total energy, and the 20 best (lowest energy) structures were used in the analysis.

## Acknowledgements

Samples of synthetic PG-1 (acetate form) were generously provided by Intrabiotics Pharmaceuticals, Inc. This work was supported by NIH grant #P01 GM 39558 to J.F., NIH grant GM 31299 to D.E., NIH grants AI37945 and AI22839 to R.I.L., and HFSPO postdoctoral fellowship to T.D.

## References

1. Kokryakov, V.N., *et al.*, & Lehrer, R.I. (1993). Protegrins: leukocyte antimicrobial peptides that combine features of corticostatic defensins and tachyplesins. *FEBS Lett.* **377**, 231–236.
2. Zhao, C., Liu, L. & Lehrer, R.I. (1994). Identification of a new member of the protegrin family by cDNA cloning. *FEBS Lett.* **346**, 285–288.
3. Zhao, C., Gains, T. & Lehrer, R.I. (1995). The structure of porcine protegrin genes. *FEBS Lett.* **368**, 197–202.
4. Qu, X.D., Harwig, S.S.L., Oren, A., Shafer, W.M. & Lehrer, R.I. (1996). Susceptibility of *Neisseria gonorrhoeae* to protegrins and defensins. *Infect. Immun.* **64**, 1240–1245.
5. Yasin, B., Harwig, S.S.L., Lehrer, R.I. & Wagar, E.A. (1996). Susceptibility of *Chlamydia trachomatis* to protegrins and defensins. *Infect. Immun.* **64**, 709–713.
6. Miyakawa, Y., *et al.*, & Catanzaro, A. (1996). *In vitro* activity of the antimicrobial peptides human and rabbit defensins and porcine leukocyte protegrin against *Mycobacterium tuberculosis*. *Infect. Immun.* **64**, 926–932.
7. Tamamura, H., *et al.*, & Fujii, N. (1995). Synthesis of protegrin-related peptides and their antibacterial and anti-human immunodeficiency virus activity. *Chem. Pharm. Bull.* **43**, 853–858.
8. Lehrer, R.I. & Ganz, T. (1990). Antimicrobial polypeptides of human neutrophils. *Blood* **76**, 2169–2181.
9. Harwig, S.S.L., Swiderek, K.M., Lee, T.D. & Lehrer, R.I. (1995). Determination of disulphide bridges in PG-2, an antimicrobial peptide from porcine granulocytes. *J. Pept. Sci.* **3**, 207–215.
10. Lehrer, R.I., Ganz, T. & Selsted, M.E. (1991). Defensins: endogenous antibiotic peptides of animal cells. *Cell* **64**, 229–230.
11. Iwanaga, S., *et al.*, & Kawabata, S. (1994). Structure–function relationships of tachyplesins and their analogues. *Ciba Foundation Symposium* **186**, 160–174.
12. Piantini, U., Sørensen, O.W. & Ernst, R.R. (1982). Multiple quantum filters for elucidating NMR coupling networks. *J. Am. Chem. Soc.* **104**, 6800–6801.
13. Briand, J. & Ernst, R.R. (1991). Computer-optimized homonuclear TOCSY experiments with suppression of cross relaxation. *Chem. Phys. Lett.* **185**, 276-285.
14. Kumar, A., Ernst, R.R. & Wüthrich, K. (1980). A two-dimensional nuclear Overhauser enhancement (2D NOE) experiment for the elucidation of complete proton–proton cross-relaxation networks in biological macromolecules. *Biochem. Biophys. Res. Comm.* **95**, 1–6.
15. Wüthrich, K. (1986). *NMR of Proteins and Nucleic Acids*. John Wiley & Sons, New York, NY.
16. Altieria, A.S., Hinton, D.P. & Byrd, R.A. (1995). Association of biomolecular systems via pulsed field gradient NMR self-diffusion measurements. *J. Am. Chem. Soc.* **117**, 7566–7567.
17. Havel, T. & Wüthrich, K. (1984). A distance geometry program for determining the structures of small proteins and other macromolecules from nuclear magnetic resonance measurements of intermolecular $^1H$–$^1H$ proximities. *Bull. Math. Biol.* **46**, 673–698.
18. Brünger, A.T. (1992). X-PLOR (Version 3.1) Manual. Yale University Press, New Haven.
19. Tamamura, H., *et al.*, & Fujii, N. (1993). A comparative study of the solution structures of tachyplesin I and a novel anti-HIV synthetic peptide, T22 ([Tyr5,12,Lys7]-polyphemusin II), determined by nuclear magnetic resonance. *Biochimica Biophys Acta* **1163**, 209–216.
20. Hill, C.P., Yee, J., Selsted, M.E. & Eisenberg, D. (1991). Crystal structure of defensin HNP-3, an amphiphilic dimer: mechanisms of membrane permeabilization. *Science* **251**, 1481–1485.
21. Lehrer, R.I., *et al.*, & Kagan, B. (1995). Protegrins: mechanism of bactericidal activity against gram-negative bacteria. *J. Invest. Med.* **43 (supp. 2)**, 288A.
22. Puglisi, J.D., Tan, R., Calnan, B.J., Frankel, A.D. & Williamson, J.R. (1992). Conformation of the TAR RNA–arginine complex by NMR spectroscopy. *Science* **257**, 76–80.
23. Terwilliger, T.C., Weissman, L. & Eisenberg D. (1982). The structure of melittin in the form I crystals and its implication for melittin's lytic and surface activities. *Biophys. J.* **37**, 353–361.
24. Leippe, M., Andra, J., Nickel, R., Tannich, E. & Muller-Eberhard, H.J. (1994). Amoebapores, a family of membranolytic peptides from cytoplasmic granules of *Entamoeba histolytica*: isolation, primary structure, and pore formation in bacterial cytoplasmic membranes. *Mol. Microbiol.* **14**, 895–904.
25. Hoffmann, J.A. (1995). Innate immunity of insects. *Curr. Opin. Immunol.* **7**, 4–10.
26. Barra, D. & Simmaco, M. (1995). Amphibian skin: a promising resource for antimicrobial peptides. *Trends Biotechnol.* **13**, 205–209.
27 Harwig, S.S.L., *et al.*, & Lehrer, R.I. (1994). Gallinacins: cysteine-rich antimicrobial peptides of chicken leukocytes. *FEBS Lett.* **342**, 281–285.
28. Sklenář, V., Piotto, M., Leppik, R. & Saudek, V. (1993). Gradient-tailored water suppression for $^1H$-$^{15}N$ HSQC experiments optimized to retain full sensitivity. *J. Magn. Reson. Ser. A* **102**, 241–245.